JOURNAL OF CATALYSIS 97, 427–436 (1986)

Crystallographic Structure and Chemisorption Activity of Palladium/Mica Model Catalysts

I. Structure and Morphology of Small Palladium Particles

M. F. GILLET AND S. CHANNAKHONE

Laboratoire de Microscopie et Diffractions Electroniques, UA 797, Faculté des Sciences et Techniques de Saint-Jérôme, Rue Henri Poincaré, 13397 Marseille Cedex 13, France

Received July 20, 1984; revised July 23, 1985

Studies carried out by transmission electron microscopy (TEM) and transmission electron diffraction (TED) on small supported Pd particles have shown that particles heated in CO + O_2 mixtures undergo changes both in morphology and in epitaxial orientation on the mica substrate. Investigations performed in bright- and dark-field TEM, before and after treatments, indicated that the changes occurring in the samples are dependent on the size of the as-deposited particles. The stabilized Pd/mica samples have well-defined structures, exhibiting a high percentage of half-cuboctahedral particles, and they can be used as good model catalysts. © 1986 Academic Press, Inc.

INTRODUCTION

A large number of investigations have been performed in an effort to understand the behavior of supported catalysts (e.g., reactivity, selectivity, poisoning). In this field single crystal surfaces have received great attention because they exhibit well-defined structures (*1–7*). However, it is not easy to correlate the bulk and surface knowledge with the catalytic behavior of a real catalyst, especially when reactions depend on the size of metallic particles. For this reason some authors have recently studied model catalysts consisting of small metallic particles condensed onto a flat insulator support (substrate). Experiments are carried out under UHV conditions combining surface analysis, chemical reaction studies, and structure determinations (*8–12*). Unfortunately, in most cases, because of the difficulties of morphological and structural investigation, the relation between the observed phenomena (in chemisorption and in catalysis) and the actual active sites often remains rather hypothetical. The present work is a contribution to this problem. We report on the structure and morphology of vapor-deposited Pd particles and the adsorption of CO. We emphasize the dependence of morphological characteristics on the adsorption properties. Our approach can be compared to the study of Doering *et al.* (*11, 12*) who have investigated CO adsorption and oxidation on Ni and Pd particles.

In this paper we first determine the growth conditions and the morphology and structure of Pd particles as a function of their size. Second, we investigate their development after heating in gas mixtures as in adsorption or oxidation experiments.

EXPERIMENTAL

Model catalysts are prepared by vapor deposition of palladium on a substrate of mica, under UHV conditions. This technique is extensively used to form epitaxial thin films, and the method is also useful to produce small metallic particles with desired size orientation and morphology. As we have shown in previous work (*13–15*) different types of metallic particles can be obtained depending on the deposition rates and the substrate temperature. We chose conditions giving tetrahedral particles in a

0021-9517/86 $3.00
Copyright © 1986 by Academic Press, Inc.
All rights of reproduction in any form reserved.

large size range with a small size dispersion (substrate temperature, 553–593 K; deposition rate, 1–2 × 10^{13} at. cm^{-2} s^{-1}). Evaporations are performed in a vacuum of 2 × 10^{-7} Pa. The mica substrate, cleaved in the atmosphere, is carefully degassed at 600 K for 1 h. The cleanliness and the crystallographic structure of the mica surface are checked by an Auger electron spectroscopy (AES)-LEED retarding field analyzer before metal deposition. The palladium source is a Knudsen cell monitored by a quartz microbalance. The deposition times are in the range 1–7 min, achieving average particle sizes between 2 and 12 nm with an average density of 1–5 × 10^{11} cm^{-2} (the apparatus is described in Part II (*16*)). The Pd deposits are investigated by transmission electron microscopy (TEM) and transmission electron diffraction (TED) using a high voltage of 100 kV. The observations are performed just after deposition or/and after thermal treatment in various gas environments (typically heating at 573 K in an O_2 + CO mixture with a partial pressure ratio P_{O_2}/P_{CO} in the range 0.1–20). Usually specimens were prepared for TEM and TED analysis by the transfer replica method: a carbon layer was deposited *in situ* on the sample and stripped off the mica substrate by floating on pure water.

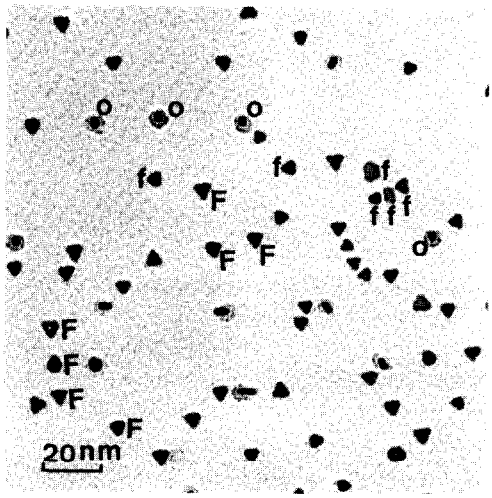

FIG. 1. Bright-field image of the Pd particles as deposited on mica (atomic flux = 1.5 × 10^{13} atoms cm^{-2} s^{-1}, T = 560 K, time deposition = 5 min).

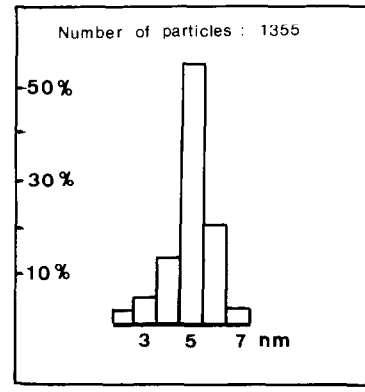

FIG. 2. Pd particle size distribution corresponding to the sample of Fig. 1.

RESULTS

Structure, Epitaxial Orientation, and Morphology of As-Deposited Particles

The bright-field micrograph in Fig. 1 shows the typical appearance of Pd particles as deposited on mica and their size distribution (Fig. 2). The substrate temperature during deposition was about 573 K. Most of the grown particles exhibit triangular outlines corresponding to tetrahedral particles. These particles have a (111) plane parallel to the substrate. Sometimes they are strongly truncated on the top and they look like triangular plates.

Figure 3a is the electron diffraction pattern corresponding to Fig. 1. It clearly shows that the particles have the (111) plane parallel to the substrate and that they are in two azimuthal orientations rotated by 30 degrees with respect to one other. Generally, the intensities of the diffraction spots relative to these two orientations are different: the more intense spots correspond to the (111) orientation called (111)F, and the other (111) orientation is called (111)f. Figure 4 shows the electron diffraction pattern of the Pd deposit together with its mica substrate. We can deduce the epitaxial relationships between the particles and their substrate as shown in Fig. 4, where Pd and mica patterns are indexed:

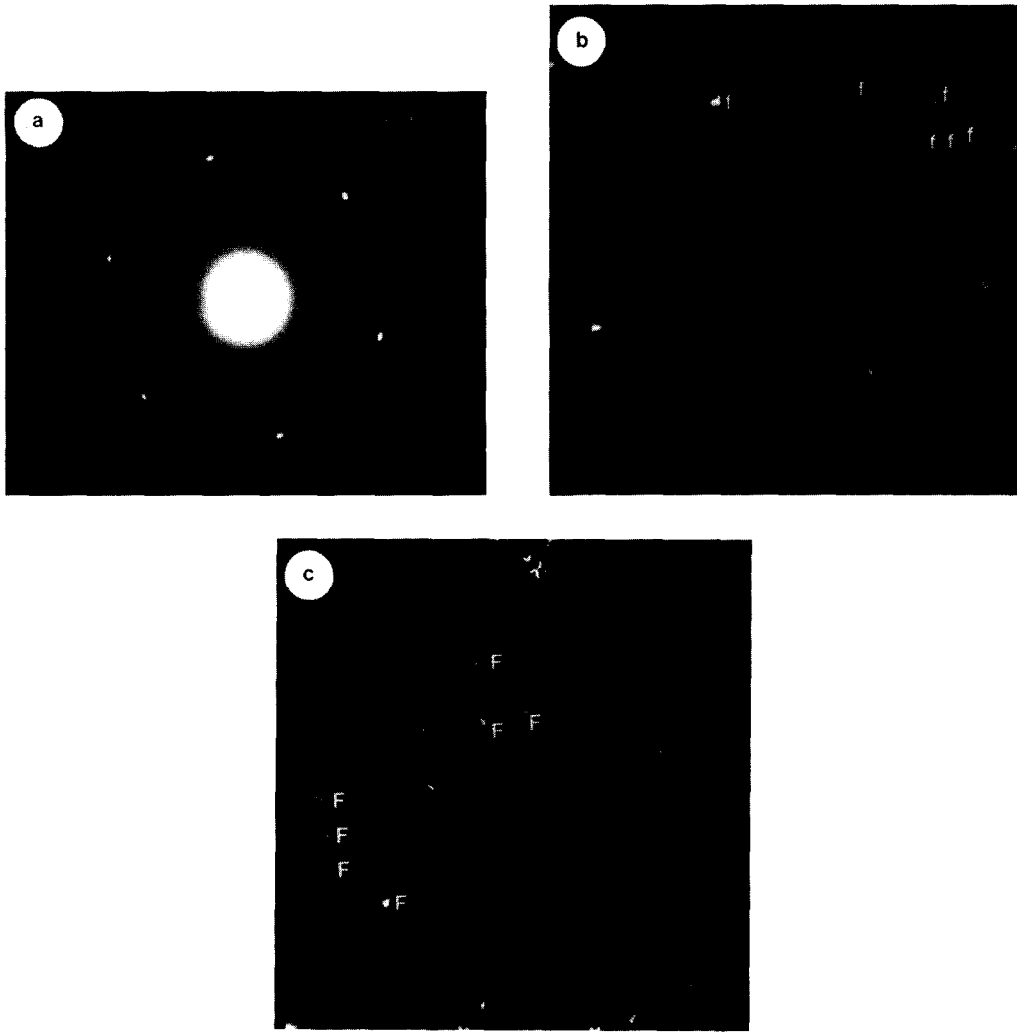

FIG. 3. (a) Electron diffraction pattern corresponding to Fig. 1. (b,c) Dark-field images of Fig. 1 obtained by the use of the (220)F and (220)f reflections, respectively.

orientation (111)F: (111)Pd//(0001)mica $[1\bar{1}0]$Pd//$[10\bar{1}0]$mica;

orientation (111)f: (111)Pd//(0001)mica $[1\bar{1}0]$Pd//$[12\bar{3}0]$mica.

The Miller indices for mica are referred to a pseudohexagonal lattice. The misfit is respectively −8% for the (111)F orientation and +6% for the (111)f orientation.

It is easy to locate on both bright-field (Fig. 3a) and dark-field (Figs. 3b and c) micrographs the crystallites belonging to each of the two (111) orientations. For each (111) orientation there are two equally probable twin related positions with the twin (111) plane parallel to the substrate. This arrangement is called "double positioning."

Some particles in Fig. 1 (marked as "○") have round shapes and are smaller than the triangular ones. These particles result from the morphological rebuilding discussed in the next section.

Structure, Epitaxial Orientation, and Morphology of Particles after Thermal Treatment

On the basis of several previously pub-

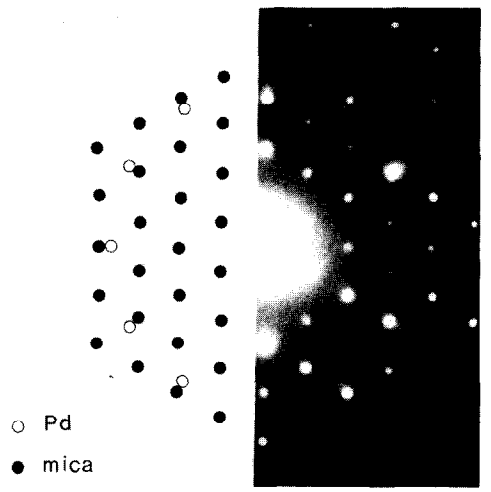

FIG. 4. Diffraction pattern from as-deposited Pd particles together with their mica substrate.

lished works on the growth and structural properties of thin vapor-deposited films it appears that the phenomena occurring after the nucleation and the growth (as crystallites migrate or coalesce) modify the population of particles (*17–21, 33*). For these reasons, before one starts with a study on a system of particles it is necessary to know the changes they undergo during an experimental run comprising thermal treatment in O_2, temperature-programmed desorption (TPD), and catalysis experiments. Thus, the as-deposited particles are heated *in situ* at 573 K in an O_2 + CO mixture for 1 h. After this treatment particles are generally very different from the particles "as deposited." Figure 5a shows a typical example of a sample after a heat treatment in O_2 + CO atmosphere (T = 573 K P_{O_2} = 1.5×10^{-4} Pa, P_{O_2}/P_{CO} = 15, time = 1 h). Figure 5b illustrates the size distribution of the Pd particles. Whatever their size, the particles are quite similar in shape; they exhibit hexagonal outlines and facets. Figure 5c is the electron diffraction pattern corresponding to the micrograph of Fig. 5a. This pattern is characteristic of treated samples with an average particle diameter less then or equal to 5 nm. It exhibits diffraction spots on the (220) ring corresponding to the (111)F and the (111)f epitaxial orientations. The reflections on the (111) and (200) rings show the existence of crystallites in two (110) orientations, $(110)_I$ and $(110)_{II}$ (Fig. 5d). It can be seen that the (111) spots located on the twofold axis of the pattern are double spots. This explains their elongated appearance. For crystallites larger than 6 nm this double reflection tends toward a single one, indicating that the two (110) orientations are twin related (*15*).

Thermal treatments in an O_2 + CO atmosphere obviously modify the morphology and the epitaxial orientation of the particles from their as-deposited state. Using dark-field techniques in TEM we are able to specify the distribution and morphology of the particles corresponding to their epitaxial orientation. For example, Figs. 6a to f show the dark-field images corresponding to the bright-field micrograph of Fig. 5a. Table 1 gives the reflections which are used for the various dark-field images and the orientation of the imaged particles.

From the dark-field images we can deduce some important conclusions:

—Most of the particles smaller than 5 nm are monocrystalline, whatever the epitaxial orientation.

—The particles are clearly three dimensional and their shape can be approximated to a half-sphere; however, they exhibit facets.

—In many cases the (111) and (110) planes of the particles, respectively, (111)

TABLE 1

Transmission Electron Microscopy (Dark Field) of Palladium Particles on Mica

Reflection	Reference to Fig. 5d	Particle orientation	Dark-field image
220	A	$(111)_F$	6a
200 + 111	B	$(110)_I$ and $(110)_{II}$	6b
111	C	$(110)_I$	6c
220	D	$(111)_f$	6d
200 + 111	E	$(110)_I$ and $(110)_{II}$	6e
111	F	$(110)_{II}$	6f

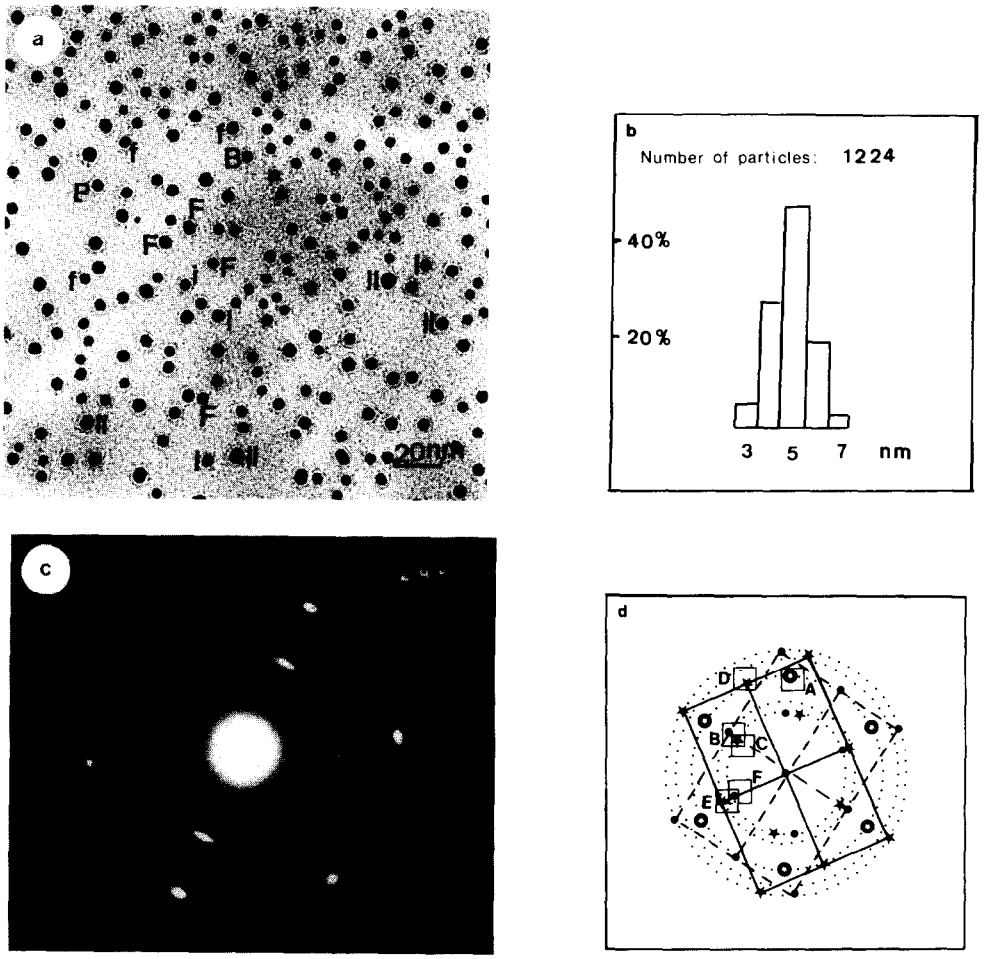

FIG. 5. (a) Bright-field image of the particles of Fig. 1 ($\phi < 5$ nm) after thermal treatment in an O_2 + CO atmosphere ($T = 573$ K, $P_{O_2}/P_{CO} = 15$, time = 1 h). (b) Corresponding Pd particle size distribution. (c) Electron diffraction pattern from Fig. 5 (a). (d) Interpretation of (c) showing the two (110) orientations.

and (110) oriented particles, are not exactly parallel to the substrate plane.

Thus, particles belonging to the same family (particles with a given orientation) exhibit differences in their contrasts. Taking this effect into account we have to use at least two dark-field images to count the total number of particles of the same family. By this means we have determined the particle density relative to the different families: for the sample corresponding to Figs. 5 and 6, in a population of 1250 particles, 470 are in (111)F orientation, 240 in (111)f orientation, and 480 in (110) orientations. Some particles (about 50) exhibit a complex structure and the smallest of them are icosahedral. The epitaxial orientation and the shape changes observed during the thermal treatments depend not only on the temperature and the nature of the gas mixture but also on the particle size. This is demonstrated by the following two examples.

The first example is illustrated by Figs. 7a and b. The micrography and the diffraction pattern are characteristic of large particles ($\phi > 5$ nm) after a heat treatment. The particles exhibit rounded or irregular shapes and their epitaxial orientations are

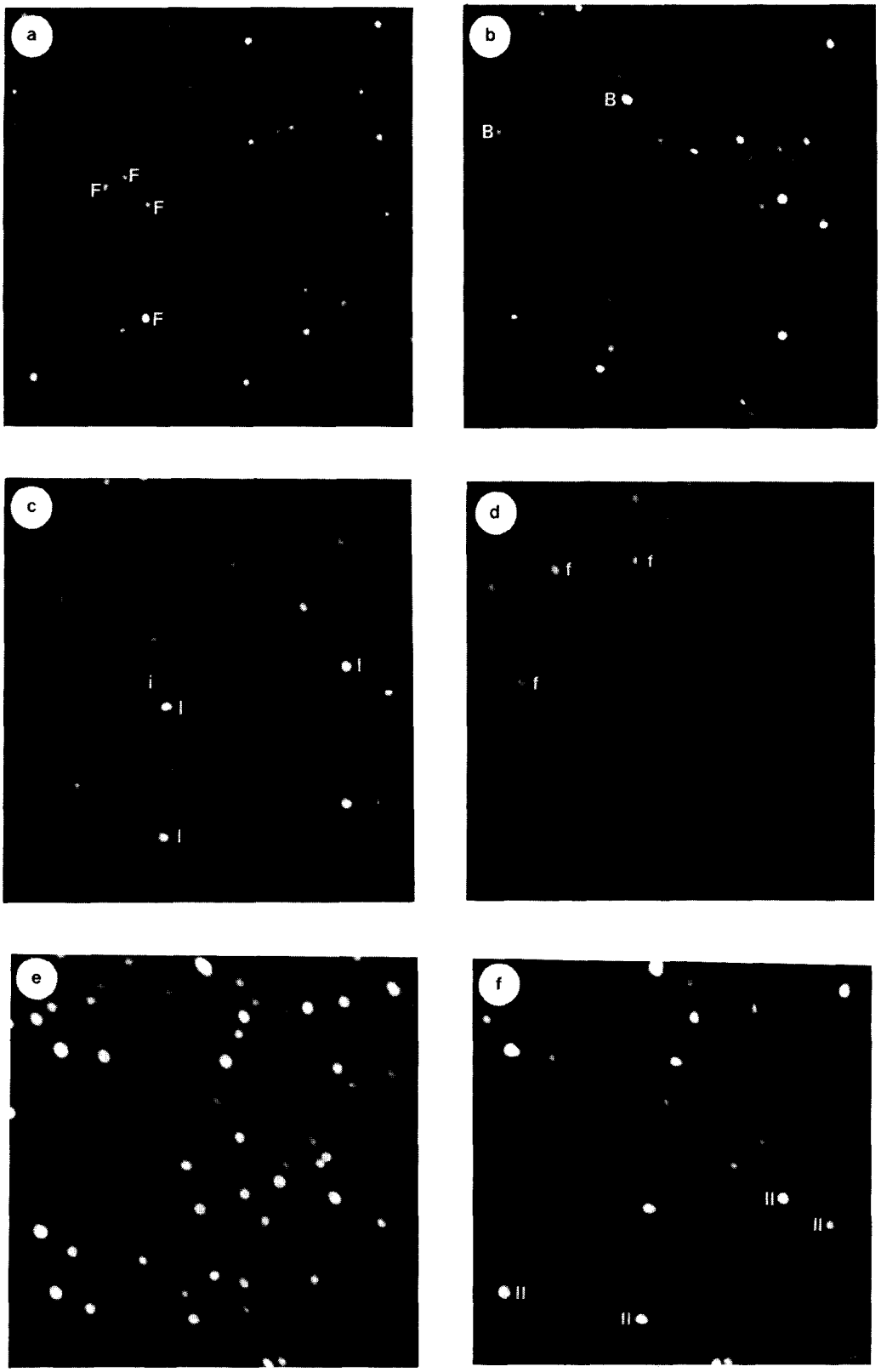

FIG. 6. Dark-field images using the reflections labeled in Fig. 5d: (a) A, (b) B, (c) C, (d) D, (e) E, (f) F.

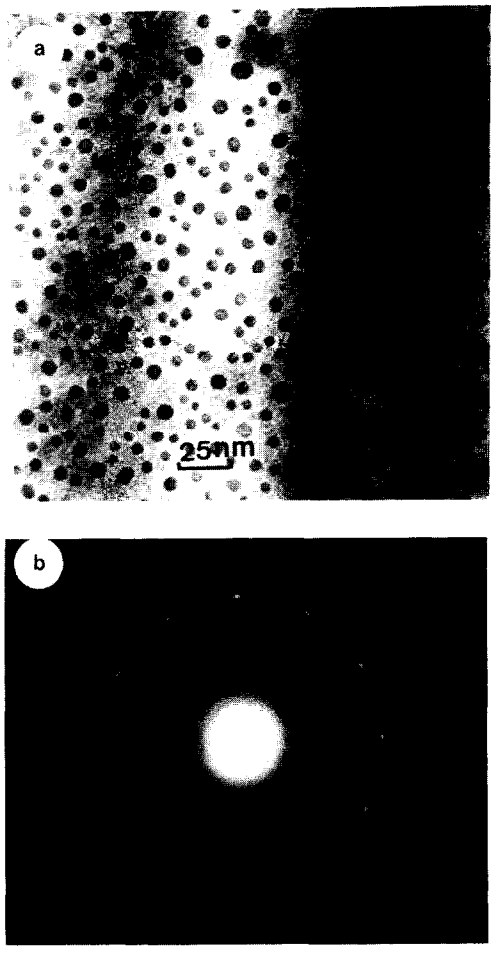

FIG. 7. (a) Bright-field micrograph of large Pd particles ($\phi > 5$ nm) after a heat treatment in CO + O_2 atmosphere (T = 573 K). (b) Diffraction pattern corresponding to (a).

the same as for the just-deposited ones. We have seen on the contrary that small particles ($\phi < 5$ nm) exhibit changes after a similar treatment (Fig. 5).

The second example concerns a deposit exhibiting a great dispersion in particle size before treatment. Figure 8a shows such a sample after a treatment (T = 593 K in a CO atmosphere for 5 min) and illustrates the influence of a treatment versus the particle size.

The dark-field images (Figs. 9a–c) performed with reflections A, B, and C, respectively (Fig. 8b), allow us to determine the crystallite families: Triangular particles T_1 (diameter > 6 nm) and hexagonal particles H (diameter > 6 nm) belong to the (III)F family. Triangular particles T_2 (4 nm < diameter < 6 nm) belong to the (111)f family and particles O (4 nm < diameter < 6 nm) belong to the (110) family. Obviously, during a treatment, when the growth is stopped, the smallest (111) particles in the as-deposited state are rebuilt in the (110) orientation. All of the rebuilt (110) particles are round but not yet faceted; this last process probably requires a longer treatment in an O_2 + CO atmosphere.

In addition, Figs. 8 and 9 illustrate two other important characteristics:

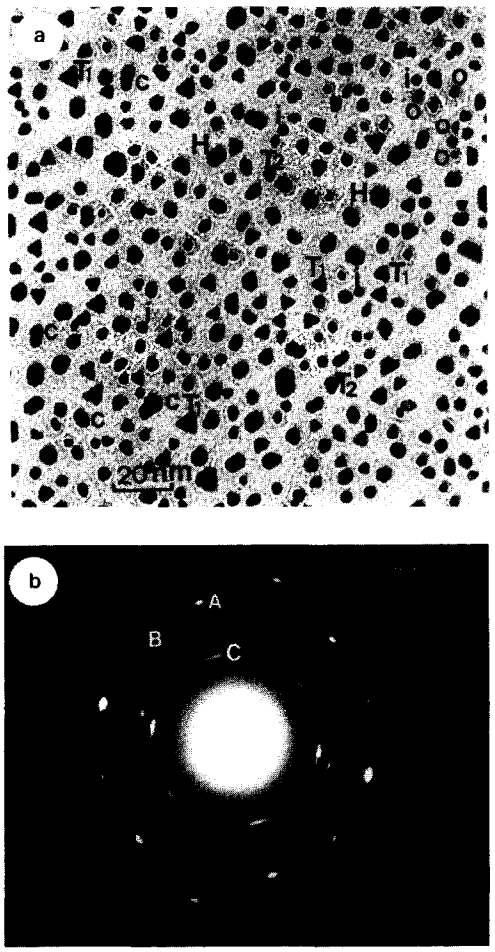

FIG. 8. (a) Bright-field micrograph of Pd particles after a heat treatment at 593 K in CO residual atmosphere. (b) Diffraction pattern from (a).

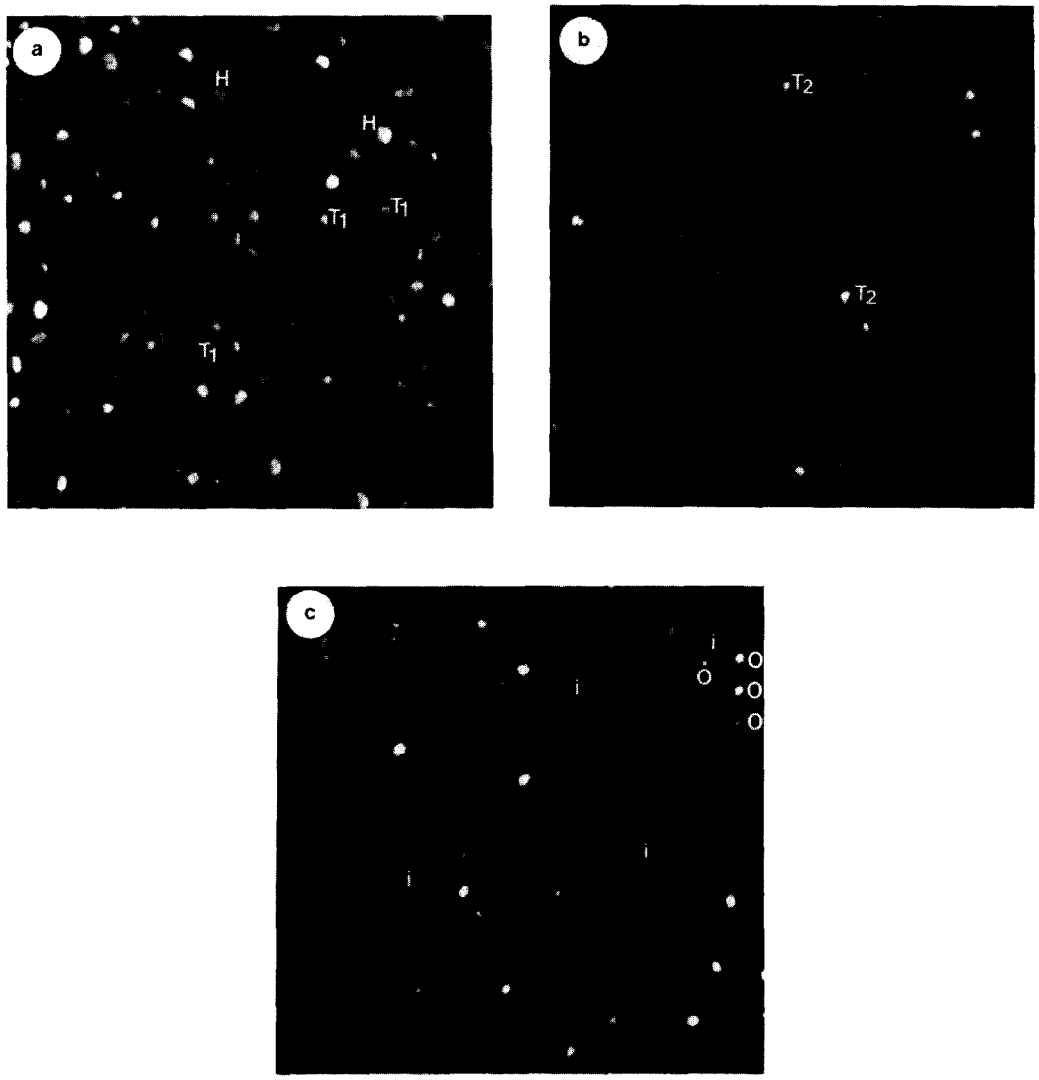

FIG. 9. Dark-field images using the reflections labeled on the pattern in Fig. 8b: (a) A, (b) B, (c) C.

(1) The dark-field images performed with (111) spots exhibit for some particles the so-called "butterfly wings" in contrast to the icosahedral structure (*22–30*). After treatment only a few icosahedral particles are visible in our samples (about 5%) (Fig. 9c).

(2) During the initial heating period, coalescence takes place. The morphology of some particles provides evidence for this process (for example, particles C in Fig. 8a).

CONCLUSIONS

Most of the as-deposited Pd particles grown in UHV on a mica substrate at 573 K are triangular plates or truncated tetrahedra. If these particles are annealed at 573 ± 30 K in an O_2 + CO atmosphere, they acquire different morphologies which depend on their size. It is not possible to specify the precise size at which a particle acquires a specific shape. However, we can give a size range for which particles with a given mor-

TABLE 2

Relation between Particle Size and Morphology

Particle size[a]	Morphology	Orientation
$\phi \leq 4$ nm	Half-cuboctahedra	(110) 40% (111) 60%
4 nm $< \phi <$ 6 nm	Half-cuboctahedra	(110) 25% (111) 35%
	Triangular or hexagonal plates	(111) 40%
$\phi \geq 6$ nm	Plates, truncated tetrahedra, half-spheres	(111)

[a] ϕ = average diameter.

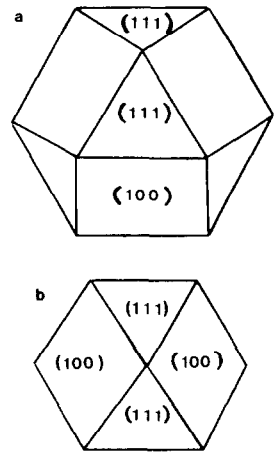

FIG. 11. Models of palladium particles smaller than 4 nm. Particles are half-cuboctahedral, (a) with a (111) plane on the mica substrate, (b) with a (110) plane on the mica substrate.

phology have a large probability of being found (Table 2).

The following conclusions can be drawn:

Size larger than 6 nm. Generally the particles have the (111) epitaxial orientation. The absence of thickness fringes seems to indicate that the particles are rather flat. The expected shape is represented in Fig. 10. They are truncated triangular or hexagonal plates, often with curved edges and corners. These particles exhibit mainly (111) free faces and small (100) facets.

Size smaller than 4 nm. The particles are three dimensional. They are faceted and are (111) and (110) epitaxially oriented. Although particles in these two orientations look very similar, they can be distinguished by dark-field images. The expected shape is a half-cuboctahedron with (111) equilateral triangular faces and the contact plane with the substrate is either (111) or (110) (Figs. 11a–b). In these two cases particles are limited by four (111) planes and three (100) planes. These two configurations differ only by their number of edges. In the (111) orientation, the particle exhibits 9 free edges while in the (110) the particle exhibits 12 free edges.

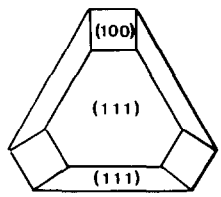

FIG. 10. Model of palladium particles larger than 6 nm.

Size between 4 and 6 nm. Such samples contain the two types of particles previously found (truncated triangular or hexagonal plates and half-cuboctahedra) in variable proportions. For example, particles of 5-nm average size exhibit 60% of half-cuboctahedra).

The particle rebuilding mechanism during annealing in an O_2 + CO atmosphere is not completely elucidated and will be discussed further elsewhere. The as-deposited triangular particles are unstable. This instability appears when the incident atomic flux is stopped. This is of great importance for the smallest particles which undergo a real rebuilding. For larger particles, the shape change is not so important and is limited to truncations and shape rounding.

In any case, the observation of the (110) orientation is indicative of morphology changes by particle rebuilding. The number of particles in the (110) orientation is about 30–40% of the total number of half-octahedral particles. It is possible, as was pointed out by Pérez *et al.* (*31*), that the half-cuboctahedra faces should not be complete, and

thus they inhibit additional edges. Under our experimental conditions, rebuilding of small particles leads to half-cuboctahedra. This process is well established for particles larger than 3 nm. Due to the observation difficulties, it is not possible to specify the exact shape of the smallest particles. However, we think that particles smaller than 3 nm acquire a more spherical shape, e.g., complete cuboctahedra. This hypothesis is in agreement with the observation of icosahedra which are quasi-spherical particles.

We think that such particle samples obtained by epitaxial growth of Pd on mica and stabilized by annealing in an O_2 + CO atmosphere are good model catalysts suitable for adsorption and catalytic reaction studies. They can be produced with high density and with a narrow size distribution. Most of them are monocrystalline with a normal fcc structure and they exhibit a simple well-defined morphology. Such collections of particles have been used for a study of CO adsorption and the results are given in Parts II and III (*16, 32*).

REFERENCES

1. Pacia, N., Cassuto, A., Pentenero, A., and Weber, B., *J. Catal.* **41,** 455 (1976).
2. Matsushima, T., *J. Catal.* **55,** 337 (1978).
3. Conrad, H., Ertl, G., and Kuppers, J., *Surf. Sci.* **76,** 323 (1978).
4. Engel, T., *J. Chem. Phys.* **69,** 373 (1978).
5. Somorjai, G. A., Chemistry in Two Dimensions. Cornell Univ. Press, Ithaca, N.Y., 1981.
6. Ortega, F., Hoffmann, F. M., and Bradshaw, A. M., *Surf. Sci.* **119,** 79 (1982).
7. Bonzel, H. P., and Krebs, H. J., *Surf. Sci.* **117,** 63 (1982).
8. Thomas, M., Poppa, H., and Pound, G. M., *Thin Solid Films* **58,** 273 (1979).
9. Ladas, S., Poppa, H., and Boudart, M., *Surf. Sci.* **102,** 151 (1981).
10. Doering, D. L., Poppa, H., and Dickinson, J. T., *J. Vaccum Sci. Technol.* **17,** 198 (1980).
11. Doering, D. L., Dickinson, J. T., and Poppa, H., *J. Catal.* **73,** 91 (1982).
12. Doering, D. L., Poppa, H., and Dickinson, J. T., *J. Catal.* **73,** 104 (1982).
13. Gillet, M., and Renou, A., *Thin Solid Films* **52,** 23 (1978).
14. Gillet, M., and Renou, A., *Surf. Sci.* **90,** 91 (1979).
15. Robinson, F., and Gillet, M., *Thin Solid Films,* **98,** 179 (1982).
16. Gillet, E., Channakhone, S., and Matolin, V., *J. Catal.* **97,** 437 (1986).
17. Heinemann, K., Osaka, T., Poppa, H., and Avalos-Borja, M., *J. Catal.* **83,** 61 (1983).
18. Metois, J. J., Heinemann, K., and Poppa, H., *Phil. Mag.* **35,** 1413 (1977).
19. Ruckenstein, E., and Chu, Y. F., *J. Catal.* **59,** 309 (1979).
20. Masson, A., Metois, J. J., and Kern, R., *Surf. Sci.* **27,** 463 (1971).
21. Kern, R., Masson, A., and Metois, J. J., *Surf. Sci.* **27,** 483 (1971).
22. Ino, S., *J. Phys. Soc. Japan* **21,** 346 (1966).
23. Allpress, J. G., and Sanders, J. V., *Surf. Sci.* **7,** 1 (1967).
24. Gillet, M., *Surf. Sci.* **67,** 139 (1977).
25. Ino, S., and Ogawa, S., *J. Phys. Soc. Japan* **27,** 1365 (1967).
26. Gillet, E., and Gillet, M., *Thin Solid Films* **15,** 249 (1973).
27. Yang, C. Y., Yacaman, M. J., and Heinemann, K., *J. Cryst. Growth* **47,** 283 (1979).
28. Heinemann, K., Yacaman, M. J., Yang, C. Y., and Poppa, H., *J. Cryst. Growth* **47,** 177 (1979).
29. Yacaman, M. J., Heinemann, K., Yang, C. Y., and Poppa, H., *J. Cryst. Growth* **47,** 187 (1979).
30. Gillet, M., Robinson, F., and Miquel, J. M., *J. Phys. Chem.* **78,** 1 (1981).
31. Pérez, O. L., Romeu, D., and Yacaman, M. J., *J. Catal.* **79,** 240 (1983).
32. Màtolin, V., Gillet, E., and Channakhone, S., *J. Catal.* **97,** 448 (1986).
33. Harris, P. J. F., Boyes, E. D., and Cairnes, J. A., *J. Catal.* **82,** 127 (1983).